Boletim de Ciências Geodésicas
ISSN: 1413-4853
ISSN: 1982-2170
Universidade Federal do Paraná

Andrade, Laura Coelho de; Ferreira, Italo Oliveira; Silva, Arthur Amaral e; Gibrim, Victoria Teixeira; Santos, Felipe Catão Mesquita

On the use of artificial neural networks in remotely piloted aircraft acquired images for estimating reservoir's bathymetry

Boletim de Ciências Geodésicas, vol. 28, no. 1, e2022006, 2022
Universidade Federal do Paraná

DOI: https://doi.org/10.1590/s1982-21702022000100006

DOI 10.1590/s1982-21702022000100006

ORIGINAL ARTICLE

On the use of artificial neural networks in remotely piloted aircraft acquired images for estimating reservoir's bathymetry

Laura Coelho de Andrade[1] - ORCID: 0000-0003-3693-2208
Italo Oliveira Ferreira[1] - ORCID: 0000-0002-4243-8225
Arthur Amaral e Silva[1] - ORCID: 0000-0001-5548-459X
Victoria Teixeira Gibrim[1] - ORCID: 0000-0002-7279-110X
Felipe Catão Mesquita Santos[1] - ORCID: 0000-0002-9376-766X

[1]Universidade Federal de Viçosa, Departamento de Engenharia Civil, Viçosa – Minas Gerais, Brasil.
E-mails: laura.andrade@ufv.br; italo.ferreira@ufv.br; arthur.amaral@ufv.br; victoria.gibrim@ufv.br; felipe.mesquita@ufv.br

Received in 23rd July 2021.
Accepted in 20th February 2022.

Abstract:

The use of acoustic systems for mapping submerged areas is the most accurate way. However, echosounders are expensive and, in addition, the equipment requires a great deal of experience on the part of the specialist. From another perspective, orbital and aerial images (acquired by RPA's- Remotely Piloted Aircraft) can offer bathymetric maps of larger locations that are difficult to access at a low operating cost. Therefore, the present study's main objective was to evaluate the utility of RGB images obtained with RPA's in water reservoirs. Thus, Artificial Neural Networks were used for depth training and prediction. Subsequently, it compared to the bathymetric data from the same pond in question, raised from acoustic sensors, quantifying the vertical uncertainty through three estimators. Regarding the statistical analysis, the RMSE and Φ estimators showed better reliability. The 300-point sample showed the best quality in processing. The results showed that the methodology could improve the management of water resources. The method allows reduced execution time and lowers cost, especially for using only the green, red and blue channels, easily found in most cameras coupled to RPA's.

Keywords: Water resources management; Submerged mapping; Remotely Piloted Aircraft; RGB images; Artificial Neural Networks.

How to cite this article: ANDRADE, L.C. et al. On the use of artificial neural networks in remotely piloted aircraft acquired images for estimating reservoir's bathymetry. *Bulletin of Geodetic Sciences*. 28(1): e2022006, 2022.

1. Introduction

Continental aquatic systems play a substantial role in maintaining biodiversity, biogeochemical regulation, the hydrological cycle, and even socioeconomic development and social well-being (BARBOSA et al.,2019). According to Ashley (2017), only 3% of the total water volume is fresh. Therefore, the management of water resources has been considered of high importance since the beginning of the 20th century.

It is known that for adequate water management, one must know the submerged relief, as well as specific information of the studied reservoir, such as the area, volume, and depth. The volume control, more specifically, can lead the researcher to develop information about the area' silting up and consequently correct or avoid possible anomalies in the water supply.

Normally, this volume is calculated through the depths acquired in bathymetric surveys, which use, in most cases, equipment called echo sounders, which are based on the principle of sound propagation in water. In addition, planialtimetric positioning systems, such as the GNSS (Global Navigation Satellite System), are also used to geo-reference depths, and inertial sensors are used to give certain control over the vessel's movements (IHO,2005; JONG et al.,2010; FERREIRA et al.,2015).

The increasing progress of technology in the hydrographic field has allowed the emergence of autonomous and unmanned sounding systems, such as the USV (Unmanned Surface Vehicle), ASC (Autonomous Surface Craft), and ASV (Autonomous Surface Vehicle). Those are quite relevant for locations that pose a risk to the crew or are shallow, in addition to the shorter time required to carry out a survey (MANLEY,2008; GIORDANO et al.,2015; FERREIRA et al.,2016).

Regarding the rise of technologies favorable to the hydrographic survey, the LiDAR (Light Detection and Ranging) system also stands out. Unlike the other equipment mentioned, LiDAR uses electromagnetic waves to estimate coastal and shallow areas' depths, acting as an active sensor. Despite this system's high cost and certain restrictions related to depth, it is important to remember that LiDAR provided even higher survey productivity, considerably reducing the field working time (GUENTHER et al., 1996; PASTOL, 2011; ELLMER et al.,2014).

In addition, orbital images used as a technique for obtaining bathymetry have been presented as a tool on the rise since the 90s (MARITORENA et al.,1994). Spectral bathymetry uses different indexes and equations to discover the best estimate compatible with the target's spectral behavior. In addition, makes it possible to monitor the studied water bodies and quantify the site's sediment (MARITORENA et al., 1994; KRUG; NOERNBERG, 2007; ZANI et al., 2009; GAUTAUM et al., 2015; FERREIRA et al., 2016).

In 1996, the author Mcfeeters (1996) proposed an index called NDWI (Normalized Difference Water Index) to delimit water bodies through combinations of bands such as green and near-infrared. In this sense, authors such as Krug& Noernberg (2007) and Ferreira et al. (2016) used this index within the Landsat and Rapideye systems, respectively, to estimate bathymetry in shallow water and obtained results with discrepancies of less than 1 meter. Furthermore, Zani et al. (2009) studied the Paraguay river using the ASTER sensor, changing the Beer-Lambert equation (SERWAY, 1983). The authors verified the band channel that had the best correlation with the data obtained in the field and thus used, posteriori, the pixel value of that band in the equation to estimate the depth.

Another technique, more recent, used to improve the bathymetry estimated by satellite images is Artificial Neural Networks or ANN. These were developed to simulate part of the human brain functioning applying mathematical equations and weighted numerical values. To correct a problem with ANN is necessary to define the best network architecture and a correct weights adjustment. According to Haykin (1999), the ANN must be configured with the type of network, adequate architecture, and adequate weights adjustment to solve a given problem, making the output vector coincide with a certain desired value. In the training process, when the network output is calculated, this response is compared with the expected output vector, and thus it is possible to find an error. Then, according to this same error, the weights are adjusted to reduce this discrepancy. Finally, the training process is repeated until the error for the set meets a minimum or previously determined value.

Authors such as Ribeiro et al. (2008) used data from the Ikonos II system combined with a hidden two-layer ANN. They proved that the methodology generates results between 0.25 m to 0.50 m maximum error, which according to the authors, meets the technical specifications of the Diretoria de Hidrografia e Navegação (DHN) for Order 1 surveys. Ceyhun & Yalçin (2010) applied an ANN to map the water depth and showed that it was efficient in estimating water bathymetry. The root mean square error (RMSEs) of ANN models for water depth detection are generalized as 0.36–4.36 m at depths of 15–18 m.

It is known that the result of the bathymetry estimated by spectral response is a mesh of points that do not represent the relief reliably. Therefore, it is recommended to use interpolators to measure the depth value in all locations (CAMARGO,1998). Commonly, geostatistics is used to estimate these unsampled values. Methods such as kriging are the most used in the literature, being universal kriging the most applied (FERREIRA et al.,2013; ANDRADE et al.,2018). It is noteworthy that the weights attribution in this method is done according to spatial and distinct analysis concerning the samples, allowing estimates without bias and with minimum variance (VIEIRA, 2000).

The emergence of uncrewed autonomous aircraft, also known as drones or UAVs (Unmanned Autonomous Vehicles) and technically as RPA's (Remotely Piloted Aircraft), meant that numerous studies related to this tool could also be carried out. For example, multispectral sensors can apply discriminant indexes for quality control and vegetation determination in agriculture, enabling better monitoring and production management. Furthermore, in the scope of hydrographic surveys, bathymetry derived from aerial photogrammetric cameras embedded in RPAs are also the subject of recent studies (AARNINK, 2017; AGRAFIOTSIS et al., 2019; ANDRADE et al., 2020). In these studies, a geometric correction should be applied due to the distortion errors existing in the image to perform equivalence between the coordinate systems of the image and the projection system (MENESES & ALMEIDA, 2012).

Andrade et al. (2020) carried out a study with RPA's. They concluded that infrared sensors could provide inputs for preliminary studies in shallow bodies of water about the morphology of the bottom of a reservoir and environmental studies, obtaining an uncertainty of 80 cm. Thus, the authors also proposed using other sensors in the image acquisition to improve the quality of the digital depth model obtained and reduce uncertainty. However, several unresolved issues are due to the few studies developed on this topic. The integration of RPAs with other sensors and performance regarding the accuracy of obtaining depths are some issues to be further explored in this area.

In this context, the present work aims to evaluate the bathymetry estimate obtained with a sensor coupled to an unmanned aircraft and apply the ANN's tool in the green, red, and blue bands.

2. Methodology

2.1 Study area

The project study area was one of the main reservoirs located at the Federal University of Viçosa (UFV) in the municipality of Viçosa, in the Zona da Mata of Minas Gerais. Such a reservoir is comprised between the latitudes 20°45'25" e 20°45'40" south, and longitudes 42°52'15 "and 42°52'30" West (Figure 1).

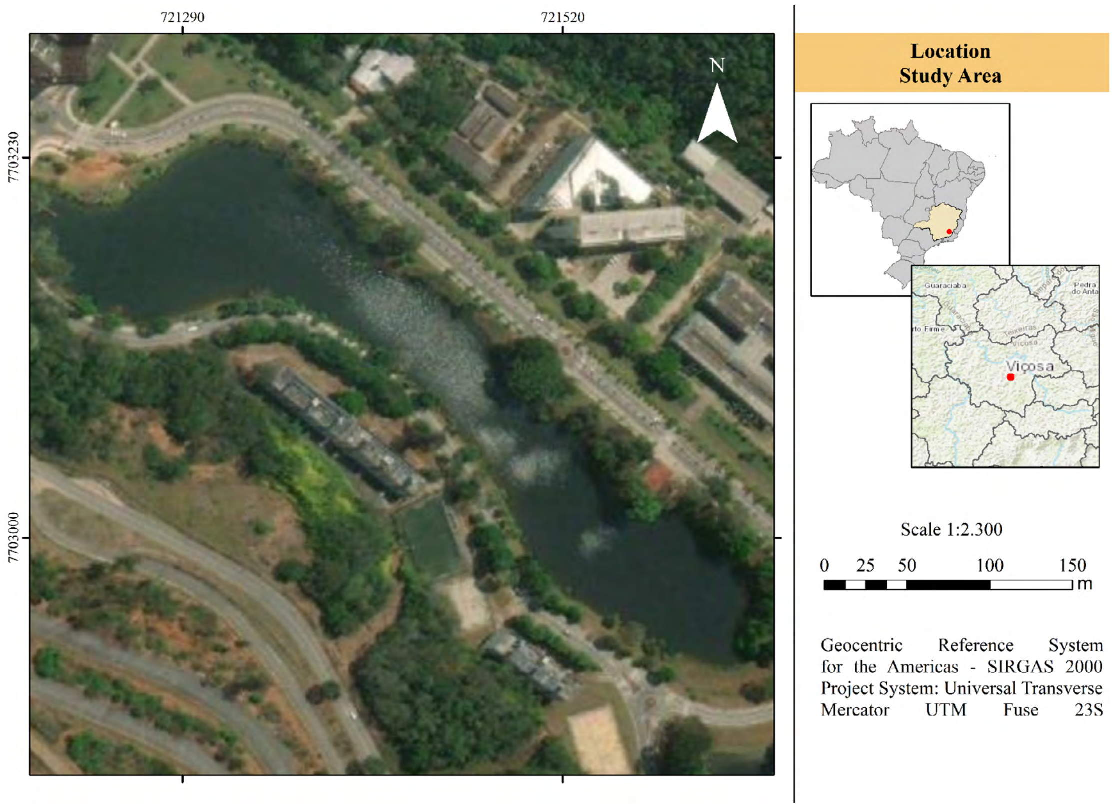

Figure 1: Study area location.

2.2 Data processing

The methodology can be better represented through the flowchart shown in Figure 2.

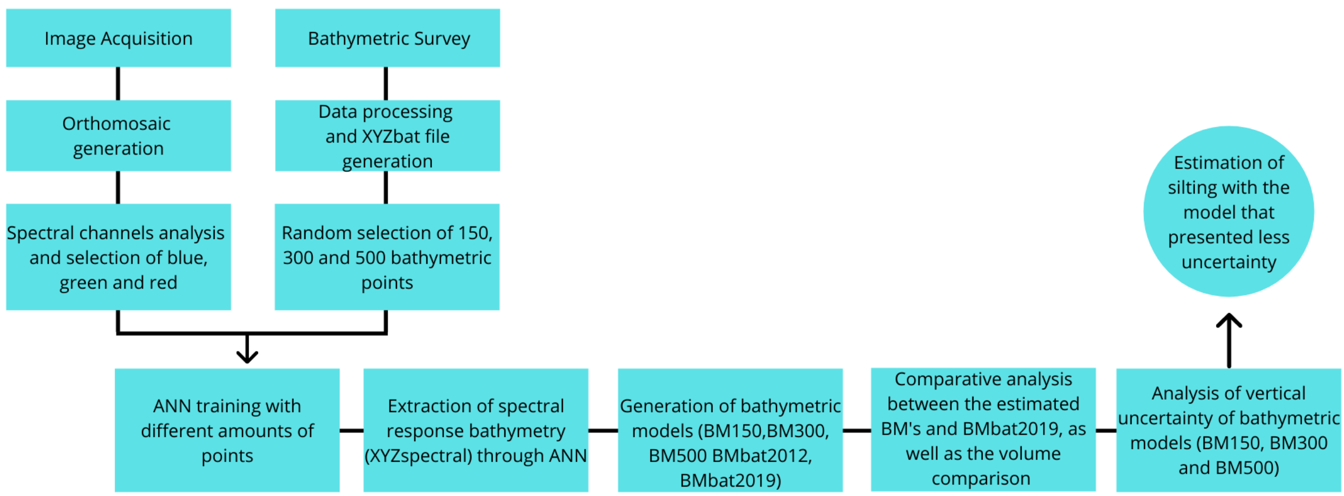

Figure 2: Methodological flowchart.

The present work used aerial images obtained by the multirotor drone Phantom 4 using a multispectral camera called Micasense. The first step was to perform the image processing, followed by the orthomosaic generation in the Agisoft software (METASHAPE, 2018).

Subsequently, knowing that the geometric correction is about the extraction of systematic errors resulting from the distortion present in the image, seven control points and another seven checkpoints located around the study area were used, collected through the GNSS Trimble R10 system. In that way, the SIRGAS2000 geodetic system and the UTM cartographic projection, zone 23s, referenced therein, were used.

The sensor used in the study has five spectral channels, namely blue, green, red, red-edge, and near-infrared (NIR), from the spectral range from 475nm to 840nm. Thus, for an adequate analysis of the generated orthomosaic, a verification was necessary to carry out the correct correlation of these bands for an analysis of the spectral behavior of the targets in the ArcGis 10.5 software (ESRI, 2019).

The determination of bathymetry through RPA's is mainly based on Beer's law. This law mentions that, due to scattering and absorption, the light that penetrates the water column is attenuated by the depth (GAO, 2009). Thus, as it is used with orbital images, one in situ data sample is also required. So, in addition, a bathymetric survey was carried out close to the flight date, following the rules proposed by ANA-ANEEL. The autonomous Echoboat-ASV system was used, which consists of a single beam echo sounder equipped with a transducer with a central frequency of 200 kHz. A GNSS receiver with Atlas Link differential correction was employed to acquire geodetic coordinates. Data collection and processing were performed using the Hypack software (HYPACK, 2018), resulting in a data file containing the points' X, Y, and Z coordinates (XYZbat). A bathymetric survey carried out in 2012 with a single-beam echo sounder by Carmo & Ferreira (2012) was also used.

Subsequently, a random selection of 150, 300, and 500 points of bathymetric data, using Arcmap's random selection method, was made for the Artificial Neural Networks training with the red, blue, and green pixels. The weights mentioned above are adjusted to achieve the intended objective during the training process, also called learning. This study case estimates the depth with green, red, and blue pixel values. In an artificial neuron, the inputs are defined by numerical values multiplied by the weights and added together to compose a single input signal (Equation 1).

$$\mathrm{S} = \mathrm{a} + \sum \mathrm{xi} * \mathrm{wi} \tag{1}$$

Where "a" is a constant value of the neuron, called "bias", "xi" represents the numerical values of the input, and "wi", the weights of each input. It is noteworthy that the weighted sum is modeled with a transfer function, which can be binary, linear, or exponential.

Currently, there are several algorithms proposed for learning neural networks. The backpropagation method is widely used in the training of ANN's of the Multilayer Perceptron type (MLP - MultiLayer Perceptron). Khadse et al. (2015) use the concept of minimizing the descending gradient and the threshold of a function.

In this study, the artificial neural network was trained and evaluated by the "neuralnet" package of software R 4.0.3, which uses the backpropagation tool in the learning process. Thus, 150, 300, and 500 samples were used, where 80% went for training and 20% for network evaluation. The network architecture had one hidden layer and only one output layer, which is the estimated depth. It should be noted that for the insertion of data in R, these had to be normalized first.

In a second step, the creation of the DDM (Digital Depth Model) was carried out for both the reference bathymetry (BMbat) and the spectral bathymetry (BMspectral). The kriging interpolation was tested between its simple and universal methods, with the universal being pointed out as the most appropriate for this type of data, as evidenced by Ferreira et al. et al. (2013), Andrade et al. (2018), and Santos et al. (2018).

For a comparative analysis between models BM150, BM300, BM500 and BMbat2012, and MBbat2019, the useful reservoir volume was calculated using ArcGIS 10.5 software (ESRI, 2019). Allowing to verify the estimate of the models found with the estimated bathymetry (BM150, BM300, BM500) and the reference bathymetry of 2019, compared to the volume in 2012.

To verify the vertical uncertainty of the model generated, all points of the reference bathymetry (from the year 2019) were selected, reduced from the estimated bathymetry for statistical analysis. It used the methodologies developed and proposed by Ferreira et al. (2018), called AEDO (Spatial Algorithm for Detecting Outliers) and MAIB (Methodology for Assessing the Uncertainty of Bathymetric Data) in an R environment (R CORE TEAM, 2020). Notably, the first methodology described has the main purpose of detecting outliers in initial data samples. Then, this sample, which the AEDO already verified, is inserted in the MAIB algorithm to assess data uncertainty statistical methods and the estimators RMSE, Uncertainty, and Robust Uncertainty. Ferreira (2018) presents further information about the MAIB algorithm.

3. Results and Discussion

From the digital values inserted in the Artificial Neural Network for training, it was possible to obtain the following network configurations for 150, 300, and 500 points, respectively (Figure 3).

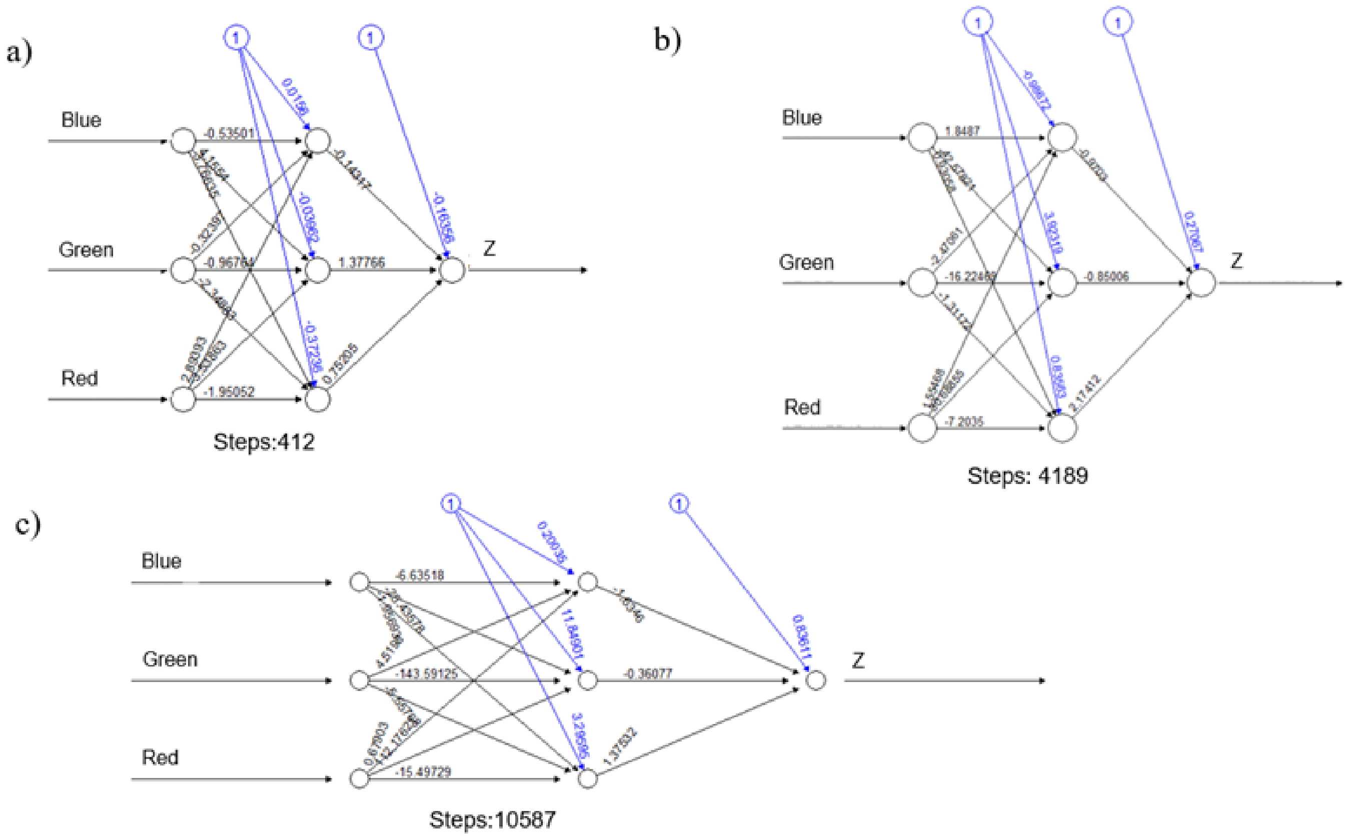

Figure 3: Neural Network Settings for a) 150, b)300 and c) 500 points in training.

As shown in Figure 3, the network contains only one hidden layer. In addition, it is important to remember that for the correct operation of the algorithm in the software, the data entered were normalized a priori. With this, the output layer called "Normalized Z" is also between 0 and 1 (Equation 2).

$$Normalized\ Z = \frac{(z - zmin)}{(zmax - zmin)} \tag{2}$$

Following the proposed methodology, geostatistical modeling based on Universal Kriging was performed. As a result, obtaining the Digital Depth Model (DDM) with better estimates for the abovementioned data sets (FERREIRA et al., 2013; ANDRADE et al., 2018; SANTOS et al., 2018). It is worth mentioning that, to obtain an excellent interpolation, it is necessary to properly model the semivariogram (SANTOS, 2015).

The digital depth models obtained by spectral bathymetry are shown below (Figure 4). Figure 5 shows the digital models obtained by traditional bathymetry in 2012 and 2019.

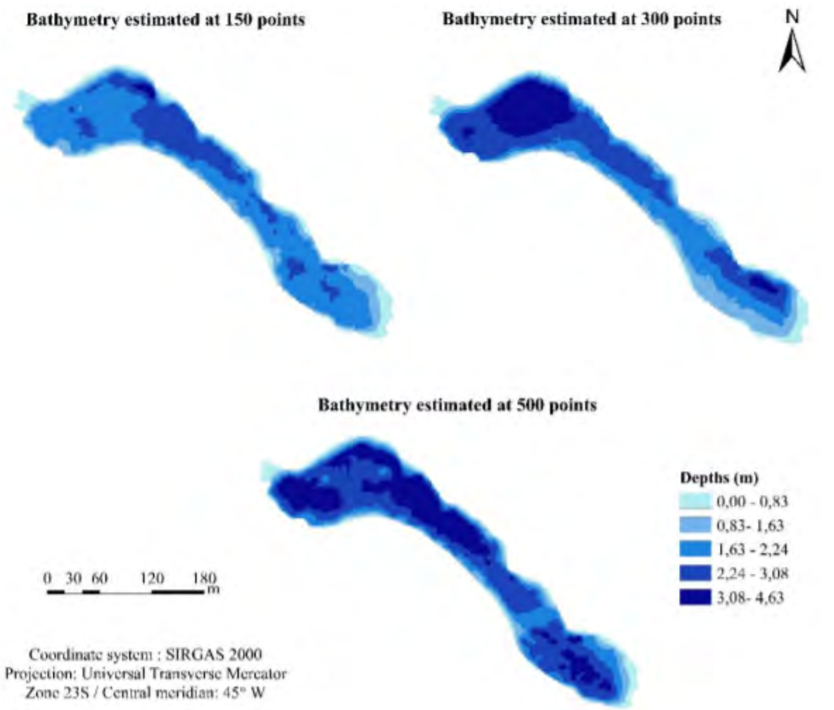

Figure 4: Digital Depth Models for 150,300 and 500 points, respectively.

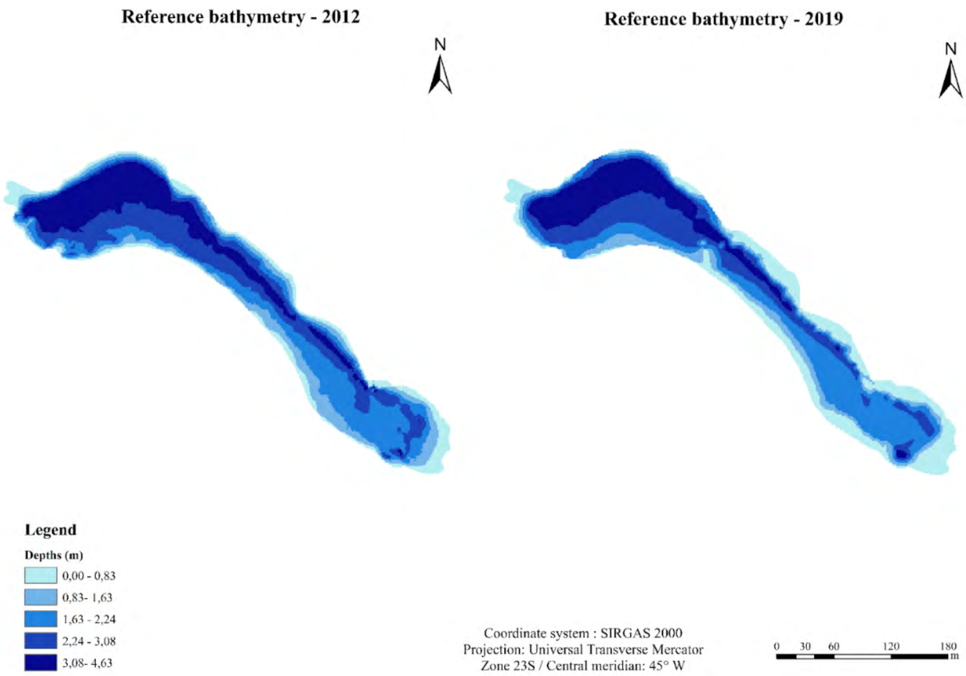

Figure 5: Digital Depth Models for the years 2012 and 2019.

From the generated models, it is possible to perceive a certain coherence with the points of greater depth, especially in the upper right part of the reservoir, which is also evidenced in BMbat2019, especially the BM500 that is the one that most visually approximates the reference model of 2019. Another fact to note is that the maximum depth in the model generated with 150 points is closer to the real (4.38 m), also shown in BMbat2019.

To carry out a quantitative comparative analysis of the models found, the volume of each one was calculated, according to the respective modeling performed (Tables 1 and 2).

Table 1: Calculated volumes of BM's for 150,300 and 500 points.

Year	**Volume (m³)**
2012	67,042.158
2019	64,611.065

Table 2: Calculated volumes of BM's of 2012 and 2019.

Training samples	**150**	**300**	**500**
Volume (m³)	57,644.72	63,963.21	66,996.81

Through the values of the existing volumes in the tables, it is possible to affirm that although the maximum depth obtained with 150 points in training is closer to the real, the volume found is the most distant from that with the use of traditional bathymetry in 2019, with a difference around seven thousand cubic meters. For 300 and 500 points, this volume showed a difference of 1 and 4%, respectively, optimal volume estimation values. To compare and assess silting in this study, the authors calculated the BMbat2012 and the volume of that same year.

For a vertical quality analysis of the generated bathymetric models, more robustly, the AEDO and MAIB algorithms were used. Furthermore, selecting all the reference points, collected through a mono-beam echo sounder, subtracted from the depth value estimated by the BM150, BM300, and BM500, so it was possible to obtain the following exploratory analysis for the discrepancies (Table 3), after passing through the AEDO algorithm.

Table 3: Exploratory analysis of discrepancies.

	150 points	**300 points**	**500 points**
Nº of observations	7,048	7,625	7,439
Mean (m)	-0.415	0.225	-0.061
Minimum (m)	-1.999	-1.207	-2.221
Maximum (m)	0.8	1.856	1.441
Variance (m²)	0.366	0.342	0.445
Coefficient of variation (%)	-145.89	259.72%	-108.94
Kurtosis coefficient	2.37	2.88	2.77
Asymmetry coefficient	-0.27	0.19	-0.25

After analyzing Table 3, it can be seen that the kurtosis coefficient is less than 3 for all analyzed sets, characterizing a platicurtic and symmetrical distribution. It is also noted, according to the variance and the variation coefficient, that the data show high variability (WARRICK & NIELSEN, 1980). Thus, it is possible to infer that the data tend to have a normal distribution.

Below, some graphs are shown to aid in exploratory analysis (Figure 6).

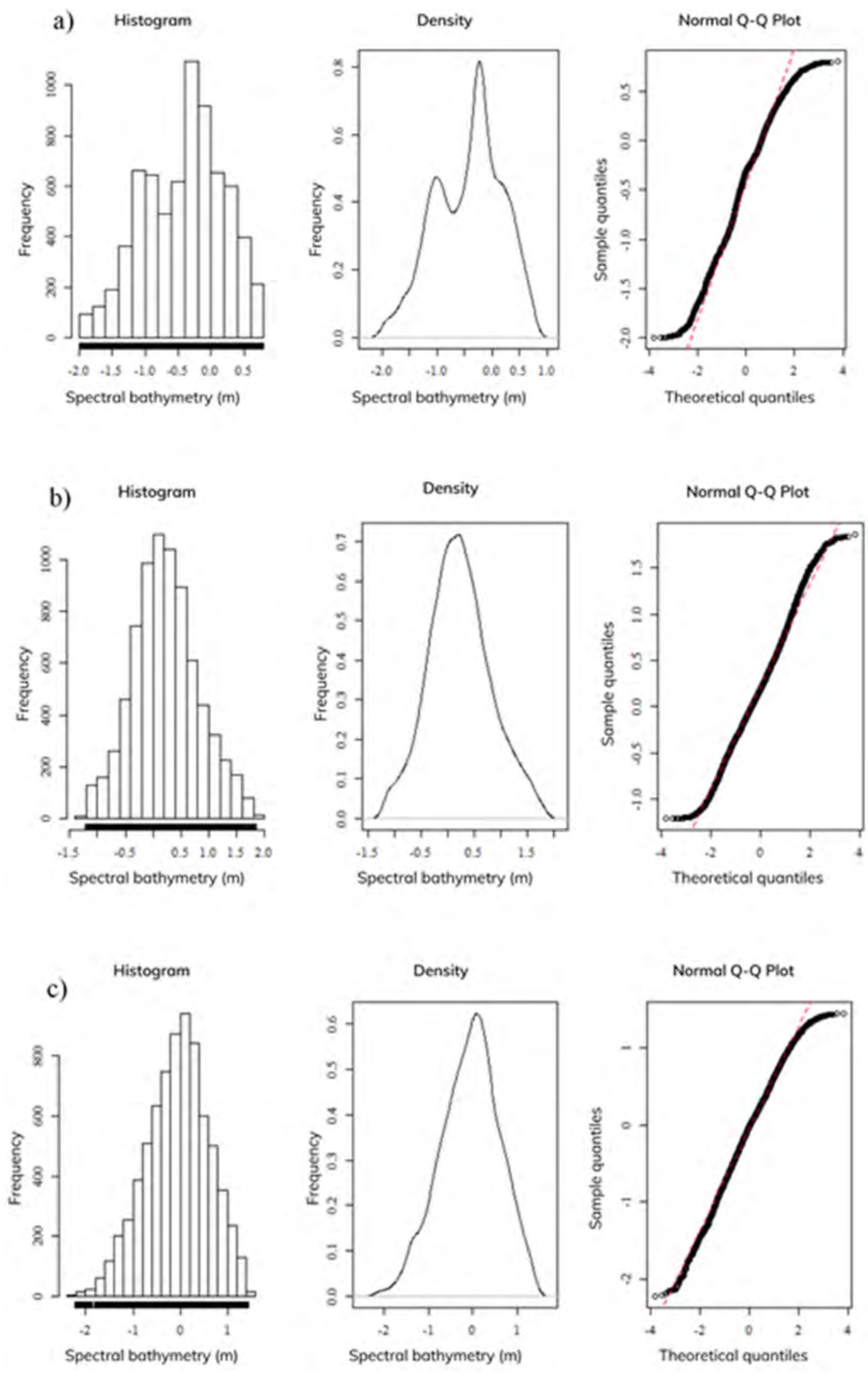

Figure 6: Exploratory spatial analysis for a) 150 training points, b) 300 training points, and c) 500 training points.

According to Ferreira (2018), the Q-Q Plot tool stands out before the histogram of the discrepancies and the density curve. It allows confirming the adequacy of the data frequency distribution to a normal distribution. After graphical analysis, it is possible to verify certain normality existing in the data since the Q-Q Plot graph is presented as an almost straight line (HÖHLE; HÖHLE, 2009). A certain abnormality is highlighted in the histogram generated with 150 training points.

Continuing with the algorithm execution, it is necessary first to examine the spatial autocorrelation and the data distribution to construct statistically good confidence intervals. According to Santos (2015), it is considered that for the application of univariate normality tests, such as Shapiro-Wilk and Kolmogorov –Smirnov, the sample must be spatially independent. Therefore, evaluating the sample spatial autocorrelation is necessary to understand the actual data normality.

Thus, the next step is the independence analysis through the experimental semivariogram (Figure 7), a tool of Geostatistics to verify this characteristic in the sample. In the methodology used, four semivariograms are constructed, with ranges equal to 100%, 75%, 50%, and 25% of the maximum distance. The analysis of these graphs concluded that the discrepancies are spatially dependent, with a strong spatial dependence for 150 points according to the classification proposed by Cambardella et al. (1994).

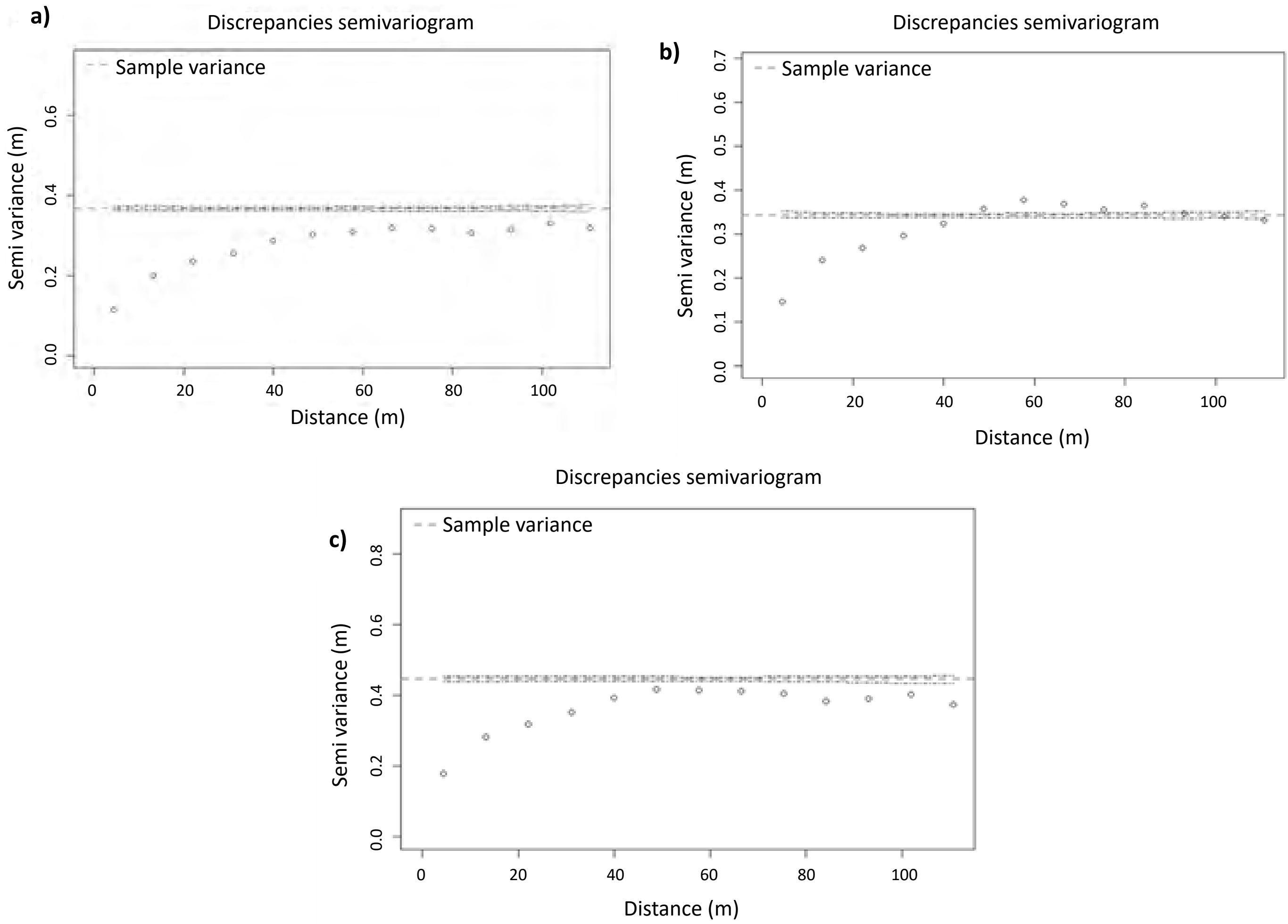

Figure 7: Experimental semivariogram for a) 150 points, b) 300 points, and c) 500 points.

After verifying data dependence, the next step following the proposed methodology consists of applying the Block Bootstrap to estimate the confidence levels. For this, 5000 replications were considered. The technique establishes 5000 new data sets and 100 as the block diagonal, corresponding to the semivariogram range. Figures 8,9 and 10 show, for 150, 300, and 500 points, respectively, the histograms and Q-Q Plot graphs of the samples built for the estimators Φ (Uncertainty), Root Mean Square Error (RMSE) and Φ_{Robust} (Robust Uncertainty), the latter being also proposed by Ferreira (2018).

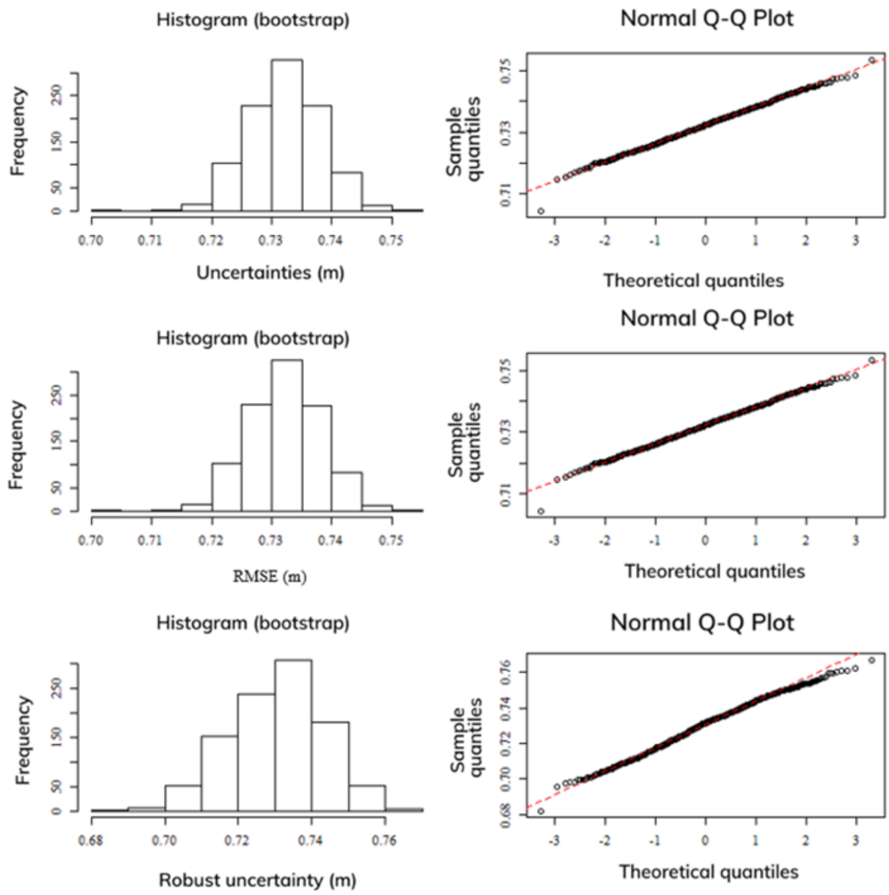

Figure 8: Histograms and Q-Q Plot charts of the Block Bootstrap sample for 150 points.

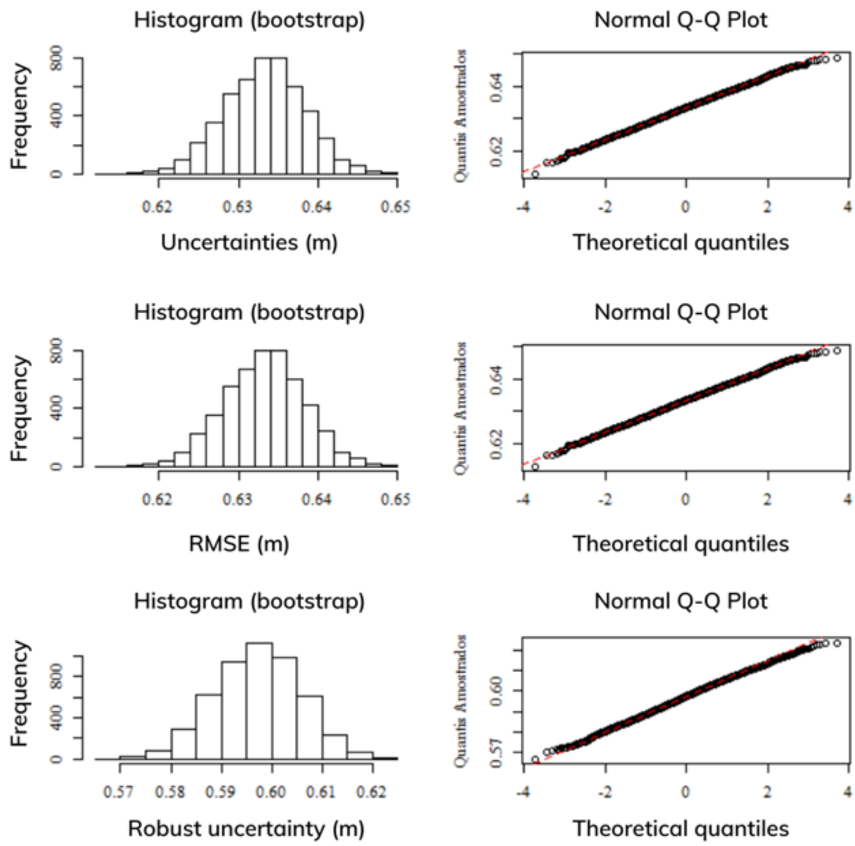

Figure 9: Histograms and Q-Q Plot charts of the Block Bootstrap sample for 300 points.

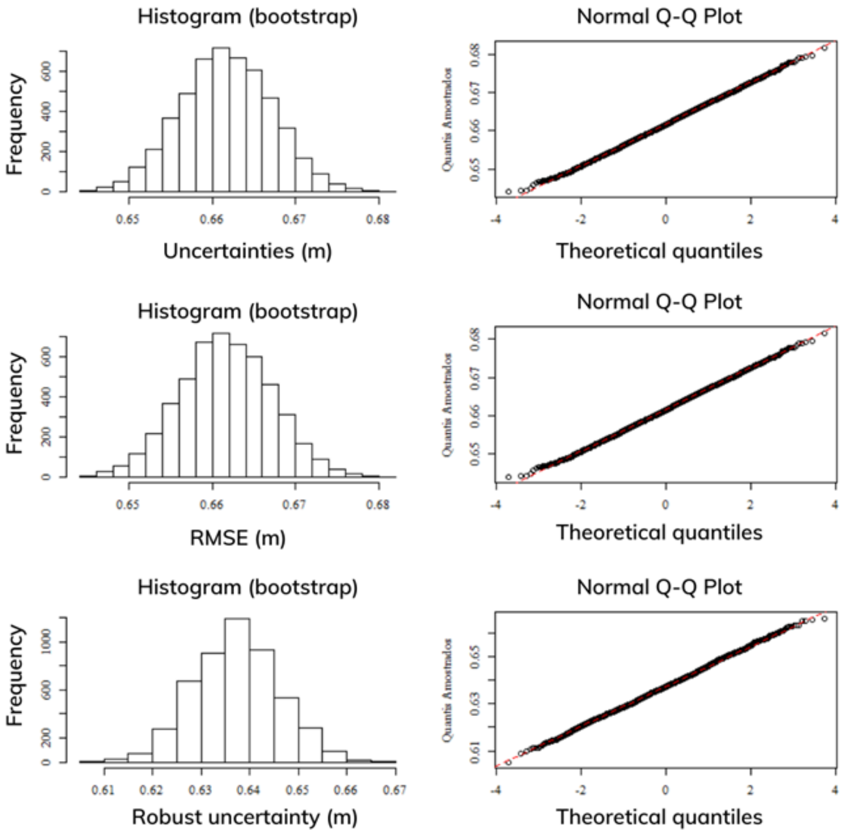

Figure 10: Histograms and Q-Q Plot charts of the Block Bootstrap sample for 500 points.

It is clear that in Figure 9, among the three estimators, Φ_{Robust} has a distribution with a lower degree of normality. However, Φ and RMSE showed a variance in the centimeter, following normality. For Figures 9 and 10, all estimators follow a normal distribution with low variances. The sample bias was also calculated to evaluate the Block Bootstrap estimates, which, according to Ferreira (2018), is determined through the difference between the uncertainty estimated using the original sample and the median of the Bootstrap data (Table 4).

Table 4: Vertical uncertainty at the 95% confidence level and Bootstrap bias.

	Estimator	**Vertical uncertainty**	**IC95%**	**Sample bias**
150 points	RMSE (m)	0.734	[0.720; 0.744]	0.001
	Φ (m)	0.734	[0.720; 0.744]	0.001
	$\Phi robust$	0.747	[0.705; 0.753]	0.016
300 points	RMSE (m)	0.627	[0.624; 0.643]	-0.007
	Φ (m)	0.627	[0.624; 0.643]	-0.007
	$\Phi robust$	0.588	[0.581; 0.613]	-0.009
500 points	RMSE (m)	0.670	[0.660; 0.681]	0.000
	Φ (m)	0.670	[0.660; 0.681]	0.000
	$\Phi robust$	0.662	[0.636; 0.671]	0.008

The Bootstrap samples generated have low values for the bias of all estimators, mainly for RMSE and Φ. It is necessary to highlight that the bias found was null for the sample trained with 500 points. However, the lowest vertical uncertainty found was for the sample trained with 300 points. In addition, it is noted that the confidence intervals are narrow, especially for the sample that was trained with 300 and 500 points, being about 2.0 cm. In this sense, it can be concluded that the estimators that best represent the variable in question are the RMSE and Φ since they present lower values for the bias and, therefore, better reliability.

Given this, it is possible to state that the sample containing 300 training points also obtained a better estimate for the reservoir volume. However, the bathymetry estimated only from the green, red and blue channels has a vertical uncertainty of approximately 0.6 m. This uncertainty can be influenced by the dense vegetation close to the banks. It is believed that this causes some inconsistencies in the digital values, making them incompatible. It is also important to note that the reservoir studied is not a clear body of water and has aquatic plants and suspended sediments that are notorious in pre-processed images.

After calculating the uncertainty and defining the best data set, the silting of the study area was estimated. Although, as described in Table 2 previously, in 2012, the reservoir had a total volume of 67,042.158 m³, for 2019, by the BM300 found by spectral bathymetry, the study area presented a volume of 63,963.21 m³, totaling a silting of approximately 3,000,00 cubic meters.

4. Conclusion

The conventional bathymetric survey is usually used for the detailed and precise characterization of the submerged relief, especially in projects that require a high degree of accuracy and greater field control.

The use of RPA's presents itself as a low-cost procedure with a shorter execution time for the determination of bathymetry, especially with the use of the green, red and blue spectral channels, which can be obtained in most aircraft. However, this tool should be carried out with caution since more tests are still needed in different areas or reservoirs with other characteristics to validate its applicability. In addition, the need to test other RGB sensors in the photographs' collection is highlighted. These also have different radiometric resolution values, which can directly affect the predicted value for the bathymetry.

Thus, it is perceived that the methodology developed in this study is valid, especially for environmental and preliminary studies. Mainly in places that do not have a high rate of suspended sediments and aquatic plants, since the understanding of spatial and temporal heterogeneities of reservoirs has great relevance to its proper management.

Another important result to be highlighted is that 300 points for training presented a product of good quality and, above all, reliable, with a difference to the real volume of only 1%.

ACKNOWLEDGEMENT

This work was carried out with the support of CAPES - Financing Code 001 and GELPH - Grupo de Estudo e Pesquisa em Levantamentos Hidrográficos at the Federal University of Viçosa.

AUTHOR´S CONTRIBUTION

Laura Coelho de Andrade contributed to the elaboration and consolidation of all phases of the manuscript under the guidance of Italo Oliveira Ferreira. The author is involved in writing and organizing the text in the bibliographic research and scientific basis.

Arthur Amaral e Silva worked in the conception of the article, in the process of discussion of the subject used in work, as well as in the translation and language revision of the manuscript.

Victoria Gibrim Teixeira and Felipe Catão Mesquita Santos participated in different stages, such as review and organization of the text, bibliographical research indications, and research materials.

REFERENCES

AARNINK, J. *Bathymetry Mapping Using Drone Imagery*. Coastal Engineering MSc thesis, Delft University of Technology, Delft, 2017.

AGISOFT L.L.C. *Agisoft Metashape*. 2018.

AGRAFIOTSIS, P. SKARLATOS, D. GEORGOPOULOS, A. and KARANTZALOS, K. Shallow water bathymetry mapping from UAV imagery based on machine learning. *arXiv* preprint arXiv:1902.10733.2019.

ANDRADE, L.C. FERREIRA, Í.O. MEDEIROS, N.G. FONSECA, I.G.R. Feasibility of using RPA's images to extract bathymetry in shallow water reservoirs. *GEOPROCESSING APPLIED TO ENVIRONMENTAL ANALYSIS*. 1ed. Editor Unesc, 2020. DOI: http://dx.doi.org/10.18616/geop06.

ANDRADE, L.C. FERREIRA, Í.O. SANTOS, F.C.M. OLIVEIRA, J.C. Evaluation of probabilistic interpolators for better water management of water bodies. *Proceedings* of the VII Brazilian Symposium on Geodetic Sciences and Geoinformation Technologies, Recife, 2018. pp.172-181.

ANEEL – ANA (National Electric Energy Agency - National Water Agency). Joint Resolution nº 003: Establish the conditions and procedures to be observed by the concessionaires and authorized hydroelectric power generation for the installation, operation and maintenance of hydrometric stations aiming at the pluviometric, linimetric, fluviometric, sedimentometric and water quality monitoring associated with hydroelectric facilities, and take other measures. Brasília - DF, 10 de Agosto de 2010.

ASHLEY, G.M. CUTHBERT, M.O. GLEESON, T.P. REYNOLDS, S.R. BENNETT, M.R. NEWTON A.C. and MCCORMACK, C.J. Hydrologic and Agent-based Modelling of Hydro-refugia in East Africa, Insights into the Importance of Water Resources in Hominin Evolution and Dispersal. In AGU Fall Meeting Abstracts.2017.

BARBOSA, C.C.F. NOVO, E.M.L. MARTINS, V.S. (1ªEd.) *Introduction to Remote Sensing of Aquatic Systems: principles and applications*. National Institute for Space Research - INPE, 2019.

CAMARGO, E.C.G. Geoestatística: Fundamento e Aplicações. In: CAMARA G., MEDEIROS J.S. *Geoprocessing in Environmental Projects*. 2ª ed. São José dos Campos: INPE, 1998. Cap 5, 36p.

CAMBARDELLA, C.A. MOORMAN, T.B. NOVAK, J.M. PARKIN, T.B. KARLEN, D.L. TURCO, R.F. KONOPKA, A.E. Field scale variability of soil properties in Central Iowa soils. *Soil Science Society of America Journal*, Madison, v. 58, n. 5, p. 1501-1511, 1994.

CARMO, E.J. FERREIRA, I.O. *Mapping the submerged reliefs of UFV's lagoons*. Technical report. Department of Civil Engineering - Surveying and Cartography Engineering Sector. Viçosa - MG.2012.

ELLMER, W. ANDERSEN, R.C. FLATMAN, A. MONONEN, J. OLSSON, U. ÖIÅS, H. Feasibility Of Laser Bathymetry For Hydrographic Surveys On The Baltic Sea. *The International Hydrographic Review*, n. 12, p. 33-50, 2014.

ESRI. ArcGIS Desktop: Release 10.5.1. Redlands, CA: Environmental Systems Research Institute. 2019.

FERREIRA, I.O. *Quality control in hydrographic surveys*. Thesis (Doctorate). Graduate Program in Civil Engineering, Department of Civil Engineering, Federal University of Viçosa, Viçosa, Minas Gerais, 216p., 2018.

FERREIRA, I. O. NETO, A. A. MONTEIRO, C. S. The use of unmanned vessels in bathymetric surveys. *Revista Brasileira de Cartografia*, v. 68, n. 10, 2016.

FERREIRA, I.O. RODRIGUES, D.D. SANTOS, G.R. Study on the Proper Use of Kriging in the Computational Representation of Bathymetric Surfaces. *Revista Brasileira de Cartografia (Online)*, Rio de Janeiro, no 65/5, p.831-842, Set/Out/2013.

FERREIRA, Í.O. RODRIGUES, D.D. SANTOS, G.R. *Collection, processing and analysis of bathymetric data*. 1ª ed. Saarbrucken: Novas Edições Acadêmicas, v. 1, 100p., 2015.

GAO, J. "Bathymetric mapping by means of remote sensing: methods, accuracy and limitations." *Progress in Physical Geography* 33(1): 103-116.2009.

GAUTAM, V. GAURAV, P. MURUGAN, P. ANNADURAI, M. Assessment of Surface Water Dynamicsin Bangalore using WRI, NDWI, MNDWI. Supervised Classification and K-T Transformation. *Aquatic Procedia*, v. 4, p. 739746, 2015.

GIORDANO, F. MATTEI, G. PARENTE, C. PELUSO, F. SANTAMARIA, R. Integrating Sensors Into A Marine Drone For Bathymetric 3d Surveys In Shallow Waters. *Sensors*, v. 16, n. 1, p. 41, 2015.

GUENTHER, G.C. THOMAS, R.W.L. LAROCQUE, P.E. Design Considerations for Achieving High Accuracy with The Shoals Bathymetric Lidar System. In: *Cis Selected Papers: Laser Remote Sensing of Natural Waters-From Theory to Practice*. International Society for Optics and Photonics, p. 54-71, 1996.

HAYKIN, S. *Neural networks. A comprehensive foundation*. New Jersey: Prentice Hall, 2 Ed. p. 842, 1999.

HÖHLE, J. HÖHLE, M. Accuracy assessment of digital elevation models by means of robust statistical methods. *ISPRS Journal of Photogrammetry and Remote Sensing*, v. 64, n. 4, p. 398-406, 2009.

HYPACK, Inc. *Hypack – Hydrographic Survey Software User Manual*. Middletown, USA, 1784p., 2018.

IHO-International Hydrographic Organization. *Manual on Hydrography*. Mônaco: International Hydrographic Bureau, 2005. 540p.

JONG, C.D. LACHAPELLE, G. SKONE, S. ELEMA, I.A. *Hydrography*. 2ª Ed. Delft University Press: Vssd, 2010, 354p.

KHADSE, C.B. CHAUDHARI, M.A. BORGHATE, V.B. Conjugate gradient backpropagation based artificial neural network for real time power quality assessment. *International Journal of Electrical Power & Energy Systems*, v. 82, p. 197-206, 2016.

KRUG, L. NOERNBERGM. Remote sensing as a tool for determining bathymetry of shallows in Baía das Laranjeiras, Paranaguá – PR. *Revista Brasileira de Geofísica*, v. 25, p. 101-105, 2007.

MANLE, J.E. Unmanned surface vehicles, 15 years of development. In: *OCEANS 2008*, IEEE, p.1-4,2008.

MARITORENA, S. MOREL, A. GENTILI, B. Diffuse reflectance of oceanic shallow waters: Influence of water depth and bottom albedo. *Limnology and oceanography,* v. 39, n. 7, p. 1689-1703, 1994.

MCFEETERS, S.K. The use of the Normalized Difference Water Index (NDWI) in the delineation of open water features. *International Journal of Remote Sensing*, v. 17, n. 7, p. 1425-1432, 1996.

MENESES, P. ALMEIDA, T. *Introduction to remote sensing image processing*. 1 ed. Brasília: UnB/CNPq, v.1, 266p., 2012.

PASTOL, Y. Use of Airborne Lidar Bathymetry for Coastal Hydrographic Surveying: The French Experience. *Journal of Coastal Research*. N. 62, P. 6-18, 2011.

R CORE TEAM. *R: A language and environment for statistical computing*. R Foundation for Statistical Computing, Vienna, Austria. URL https://www.Rproject.org/.2020.

RIBEIRO, S.R.A. CENTENO, J.A.S. KRUEGER, C.P. Depth estimation from bathymetric survey and IKONOS II data using artificial neural network. *Bulletin of Geodetic Science*, v. 14, n. 2, p. 171-185, 2008.

SANTOS, A.P. 2015. *Cartographic quality control: methodologies for assessing positional accuracy in spatial data*. Thesis (PhD). Graduate Program in Civil Engineering, Department of Civil Engineering, Federal University of Viçosa, Viçosa, Minas Gerais, 172p.

SANTOS, F.C.M. FERREIRA, I.O. ANASTACIO, L.C. OLIVEIRA, J.C. Use of optical remote sensing to estimate the silting up of water reservoirs. In: Brazilian Symposium on Geodetic Sciences and Geoinformation Technologies, 2018, Recife. *Anais* do VII SIMGEO. Recife: Editora UFPE, 2018. v. 1. p. 936-944.

SERWAY, R.A. *Physics for Scientists and Engineers*. CBS, p.132-133,1983.

VIEIRA, S.R. Geostatistics in studies of soil spatial variability. In. NOVAES, R.F. ALVAREZ, V.V.H. SCHAEFER, C.E.G.R. *Topics in soil science*. Viçosa, MG: Brazilian Soil Science Society, v.1. p.2-54, 2000.

WARRICK, A.W. and NIELSEN, D.R. Spatial variability of soil physical properties in the field. In: HILLEL, D. *Applications of soil physics*. New York: Academic Press, p.319-344, 1980.

ZANI, H., ASSINE, M.L. SILVA A. Fluvial bathymetry estimated with orbital data: a case study in the Upper Course of the Paraguay River with the aster sensor. *Geociências (São Paulo)*, v. 27, n. 4, p. 555-565, 2008.